Open Chem., 2015; 13: 549–556

Research Article **Open Access**

Péter Fazekas*, Anna Mária Keszler, Eszter Bódis, Eszter Drotár, Szilvia Klébert, Zoltán Károly, János Szépvölgyi

Optical emission spectra analysis of thermal plasma treatment of poly(vinyl chloride)

Abstract: Decomposition of poly(vinyl chloride) (PVC) was investigated in radiofrequency thermal plasma in neutral, oxidative and reductive conditions. Optical emission spectroscopy (OES) was applied for the characterization of the plasma column. OES was used to identify active plasma components such as excited atoms, ions, radicals and molecules. The spectra were dominated by molecular C_2, CN, OH, and CH bands, and atomic H, Ar, C, Cl and O lines. Emission intensities of main species were monitored versus various experimental parameters. The rotational-vibrational temperatures determined from different bimolecular species were considered in the range of 2000–6400 K. Solid soot samples were collected and purified to investigate the possibility of graphene formation as a by-product of the decomposition process.

Keywords: Poly(vinyl chloride), PVC, Thermal Plasma, Optical Emission Spectroscopy

DOI: 10.1515/chem-2015-0069
received January 20, 2014; accepted May 30, 2014.

1 Introduction

Poly(vinyl chloride), abbreviated as PVC, is one of the most manufactured plastics, its production is more than 31 million tons per year [1]. Its applications are widespread and it is commonly used as window frames, pipes, bottles, cables, wires, wallpapers and imitation leathers [2].

The increasing demand on its production has put the problem of waste PVC into spotlight. It is a stable material, which does not decompose; therefore its storage in landfills requires more and more territory. Several technologies have been proposed for recycling of disposed PVC but they have not reached a reassuring solution yet [3]. Mildly thermooxidative conditions led to polymer chain fragmentation and the decrease in molecular mass [4]. The thermal destruction of this plastic via conventional high temperature decomposition processes such as pyrolysis or cracking results in toxic by-products, which are stable and also have adverse effects on human health and on the environment as well. In neutral conditions benzene formation is significant: after the elimination of HCl from the polymer chain ring closing reactions take place [5-7]. During incineration the presence of several types of dioxins and furans are reported [8]. Thermal plasma treatment offers an environmental benign solution due to its special properties. The extremely high temperature (8000–10000 K) and strong UV radiation induces great number of reactive species. The high quenching rate (~10^6 s K^{-1}) helps to avoid the recombination of radicals into large, stable molecules [9]. It has been used previously with success to decompose both polymers [10] and chlorinated organic molecules [11-12].

The downside of thermal plasmas is their high operation costs. If the end products of the processes contain some utilizable materials, these costs could be lowered. During plasma treatment of carbon containing materials several nanostructures can be formed. From graphite precursor fullerenes of various sizes were produced in thermal plasma [13]. The production of mono and multilayer carbon nanotubes are one of the most thorough researched topics today [14-16]. Industrial diamond can be synthetized from chlorobenzene [17]. It is also known from literature that growth of graphene layers can be observed during the thermal treatment of PVC at 600–1000°C [18].

***Corresponding author: Péter Fazekas:** Institute of Materials and Environmental Chemistry, Research Centre for Natural Sciences, Hungarian Academy of Sciences, Pusztaszeri Street 59-67. Budapest, Hungary 1025, E-mail: fazekas.peter@ttk.mta.hu
Anna Mária Keszler, Eszter Bódis, Eszter Drotár, Szilvia Klébert, Zoltán Károly, János Szépvölgyi: Institute of Materials and Environmental Chemistry, Research Centre for Natural Sciences, Hungarian Academy of Sciences, Pusztaszeri Street 59-67. Budapest, Hungary 1025
János Szépvölgyi: Research Institute of Chemical and Process Engineering, University of Pannonia, Egyetem Street 10. P.O. BOX 10, Veszprém, Hungary 8200

Table 1: Tests conditions.

Run	Feed rate (g h^{-1})	Auxiliary gases (stoichiometric ratio)	C_2 temperature (K)	OH temperature (K)	CN temperature (K)
Run-1	50	—	6400	—	5000
Run-2	100	—	5000	—	5400
Run-3	150	—	4600	—	6200
Run-4	50	0,5 O_2	4000	5000	—
Run-5	50	1 O_2	3400	4900	—
Run-6	50	2 O_2	2000	4700	—
Run-7	50	0,5 H_2	5100	—	5300
Run-8	50	1 H_2	4700	—	4900
Run-9	50	2 H_2	4000	—	6200

In this paper we report on the decomposition of PVC as a model compound of chlorinated polymers in an inductively coupled radiofrequency plasma reactor in neutral, oxidative and reductive conditions. We investigated both the generated chemical species and fragments in the plasma, and the obtained solid materials after the decomposition, as well. The chemical species of the plasma column was monitored and analysed by optical emission spectroscopy (OES). OES is a convenient method for monitoring plasmas because chemical species can be identified and various parameters, such as temperatures, can be determined without any interference on the plasma state. Also, the optical emission measurements of the Swan system of C_2 ($d^3\Pi_g$ – $a^3\Pi_u$) transition are commonly used as a diagnostic tool for carbon plasmas [19-21]. The as-collected solid materials were analysed by transmission electron microscopy (TEM) to investigate the possible graphene formation and to verify the total decomposition of the fed material.

2 Experimental Procedure

2.1 Experimental set-up

The experimental set-up consisted of a RF inductively coupled plasma torch (TEKNA PL 35) connected to a high frequency (4-5 MHz) LEPEL generator, a reactor, a cyclone, a filter unit and a vacuum pump. The cylindrical reactor was made of stainless steel with an inner diameter of 19.7 cm and length of 121.6 cm. The pressure in the chamber was atmospheric during the experiments and the generator operated at 20 kW in each run. The PVC powder for the tests was provided by BorsodChem Co. (Hungary). It contained no additives and had an average particle size of 150 μm. It was injected to the top of the plasma column with feed rates of 50–150 g h^{-1}. Ar was used as carrier gas of 9.4 dm^3 min^{-1} flow rate. The plasma torch was also operated with Ar central gas and Ar sheath gas with flow rates of 15.5 dm^3 min^{-1} and 35.5 dm^3 min^{-1}, respectively. In certain runs O_2 or H_2 was also added into the sheath gas with varying stoichiometric concentrations. The experimental conditions are listed in Table 1. The reactor was made of stainless steel with the inner diameter of 19.7 cm and length of 121.6 cm. The scheme of the plasma system is specified elsewhere [22].

2.2 Plasma emission spectroscopy

Plasma emission was collected at two spots, 70 and 180 mm far from the most bottom turn of the inductive coil, perpendicularly to the axis of the plasma column through quartz view ports. The wavelength was selected by a 55 cm focal length monochromator (Jobin-Yvon TRIAX 550) having 1200 grooves mm^{-1} grating. Light was collected and transferred to the entrance slit by a multi-legged fibre optics. Plasma emission was detected by an optical multi-channel analyser (CCD-3000). The spectral range and the FWHM (full width at half maximum) were 200–1000 nm and 0.2 nm, respectively. The step resolution was 0.025 nm. Assignation of atomic lines was performed on the base of information tabulated in NIST Atomic Spectral Database [23], while molecular bands were identified on the base of spectroscopic information available in the spectral simulation code LIFBASE [24] and in the published literature [25-27].

2.3 Solid product analysis

To monitor the incidental residual PVC fragments and to investigate the possible graphene formation during the PVC decomposition, the soot was recovered from the wall of the plasma reactor. For graphene determination soot was purified (100 mg) with boiling (150°C) 30 wt.% H_2O_2 (10 cm^3) trough 5 hours to remove amorphous carbon particles [28]. Soot particle morphology of the as-obtained materials and unpurified samples were characterized by scanning electron microscopy (SEM, Zeiss EVO 40XVP), transmission electron microscopy and selected area electron diffraction (TEM and SAED, Morgagni 268D).

3 Results and Discussion

3.1 Thermodynamic calculations

In order to forecast degradation processes and their products, thermodynamic calculations were performed in the temperature range of 500–7000 K using the computer code FACTSAGE that is based on the minimization of Gibbs free enthalpy. Ideal gas conditions could be reasonably assumed because of the near atmospheric pressure and high temperature conditions found in this plasma type [14]. The calculations were performed for three different systems: neutral, reductive (PVC + $2H_2$) and oxidative conditions (PVC + $2.5O_2$).

In neutral conditions the degradation products could be sorted into three groups. H, C and Cl atoms were the main products over 5000 K. Below 3000 K HCl, H_2, CH_4 molecules and solid C were dominant. Between 3000 and 5000 K small carbon clusters (C_2, C_3, C_4, C_5), C_2H_2, various hydrocarbon radicals (CH, CH_2, CH_3, C_2H, C_2H_2) and some chlorinated compounds (CCl, C_2Cl, C_2HCl) appeared. At lower temperatures HCl was the only chlorine containing molecule, and the formation of Cl_2 was not relevant (Fig. 1a).

The results of reductive condition were very similar. The amount of H and H_2 increased for evident reasons and at the same time the production of C_4 and C_5 clusters was supressed.

In the presence of oxygen, no CH_4, solid C or any of the whole third group could be detected. C_2 and CH remained but only above 6500 K. Gaseous C appeared also only around 5000 K, H_2 molecule disappeared below 1500 K. The main carbon containing compounds became CO_2 and CO. In the 3000–4000 K region O_2 and OH were abundant. At the same place oxygen containing species

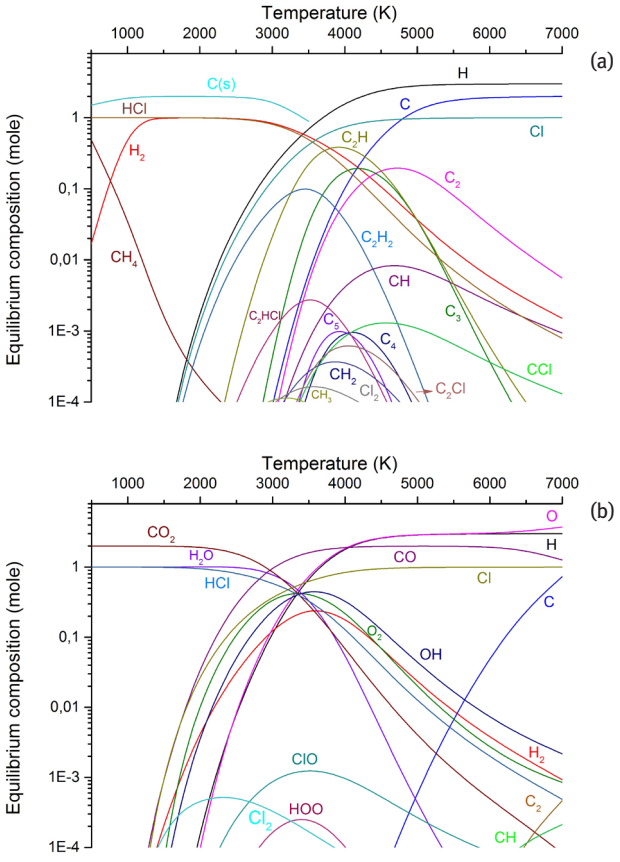

Figure 1: Thermodynamic calculations for thermal decomposition of PVC in neutral (a) and oxidative (b) conditions.

were observed, such as HOO and ClO (Fig. 1b). Although Cl_2 got more dominant with higher concentration and wider temperature interval, HCl remained the main chlorine containing molecule.

3.2 Identification of atomic and molecular active species in plasma phase

Each of the plasma zones is clearly defined by its emission spectral fingerprints, containing several atomic transitions and molecular electronic bands. The upper part of the plasma column observed 70 mm beneath the torch was featured by strong emissions of Ar, H, C, Cl and O atomic line transitions (Fig. 2). These emission lines were very weak or not detectable at the lower view port. Spectral lines of Ar atom (Ar I) in the 700–850 nm range and ion (Ar II) between 300–350 nm wavelengths were detected in each experimental condition. The hydrogen lines of the Balmer series as alpha and beta lines (H_α = 656.28 nm; H_β = 486.1 nm) can be clearly distinguished. These

hydrogen lines are present in almost all hydrocarbon flames and are extremely bright, with the H_α line being the strongest. The H_β line (Fig. 3) showed broadening which is attributed to Stark broadening [29]. Chlorine atomic lines (Cl I) were observed at 725.6, 754.7, 822.2 and 912.2 nm. Oxygen lines (O I) at 777.2, 777.4 and 777.5 nm appeared in spectra when oxygen was introduced in the plasma. Weak carbon atomic (C I) lines were recorded at 477.2, 538.1 and 600.2 nm. Several ionic lines were observed in the spectra in neutral conditions between 270 and 400 nm. These lines were identified mostly as carbon ionic (C II) transitions, for example at 299.2, 391.8 and 392.1 nm. Few Ar II and Cl II lines were observed at 297.9, 349.2, 374.6, 394.6 nm and at 335.3, 380.5 and 386.1 nm, respectively. Further C II lines were found at 588.8 and 589.3 nm. Atomic O, C, and H radicals can initiate further plasma chemical reactions, and contribute to formation of other radicals and reactive species such as HO, HOO and C_2O. In some cases metallic atomic lines, as Zn I at 330.1, 334.4, 481.1 nm were detected as well. These lines appeared due to metal content of inhibitors or initiators used in the polymerization processes.

Molecular emission systems were observed at both view ports (Fig. 2). Three key molecular species were present in neutral and reductive conditions in various exited states: C_2, CH and CN. The formers were produced by the electron impact dissociation of PVC and it led to the emission of the Deslandres-d'Azambuja and Swan systems for C_2, and the 4300 Å and 3900 Å system of CH respectively. In neutral and reductive atmosphere strong features for the CN Violet band centring at 388 nm could be observed. The CN molecule originated as a result of reactions of diatomic carbon (C_2) or hydrocarbons, formed during the decomposition process, and active nitrogen species. The presence of nitrogen could be explained by the impurity of the Ar gas or with a small leak in the system. Also what we observed was very weak and noisy, thus rather uncertain sings of the Fulcher band of the H_2 molecule between 595–630 nm in our spectra. Oxidative conditions give rise to OH radical.

An unknown band system was observed in the range of 700–1150 nm, which was attenuated in reductive conditions but was missing completely in oxidative conditions. This band system was identified as the second order CN violet system [30].

There are some other molecular bands, which are commonly observed in carbon plasmas. The C_2 Phillips system (750–1200 nm) was observed in heavy-current discharges and is known to be a strong feature in most carbon systems including arcs and flames [25]. Also the CN molecule has another rotational-vibrational system beside

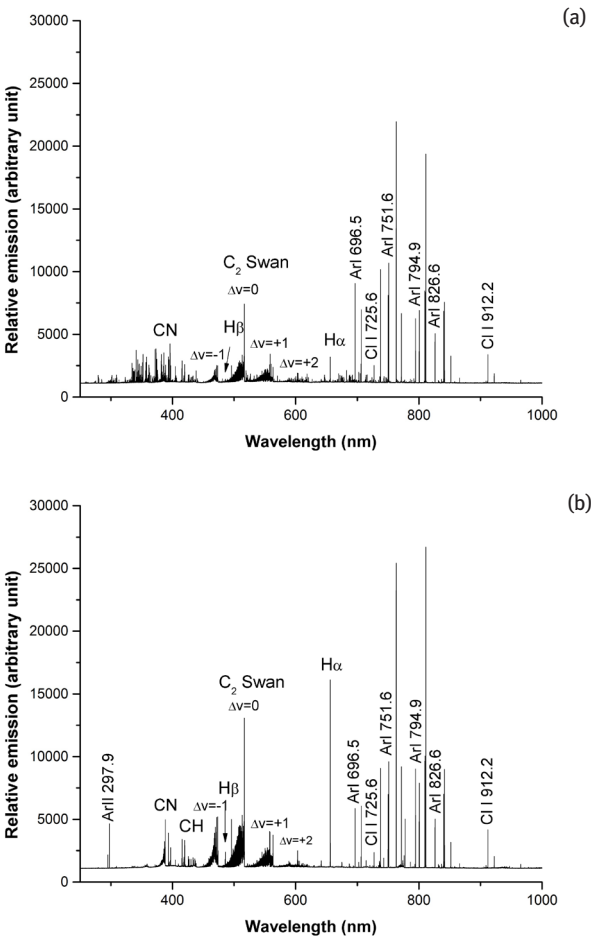

Figure 2: Optical emission spectra of the plasma during PVC decomposition in neutral (Run-1) (a) and reductive (Run-8) (b) environment recorded 70 mm beneath the torch.

the Violet one and it can be observed in the 600–1000 nm region (Red band). Furthermore, it would be possible theoretically to find three-atomic molecules formed of carbon and nitrogen (such as CNN, NCN or CCN) emitting in this wavelength interval, but their electronic spectrum tends to appear in the far ultra-violet region [31]. However, none of these bands appeared in our spectra. The detected molecular systems are summarized in Table 2.

Increase of the H_2 concentration in the plasma column resulted in more intensives hydrogen lines (H_α, H_β), C_2, and CN bands, while other atomic lines such as C and Cl could be sparely detected. The intensity of CH band increased significantly and in parallel the ionic carbon lines (C II) in the 270–400 nm region disappeared entirely. Both phenomena can be explained with a reaction between carbon and hydrogen, which were observed in high temperature systems [32]:

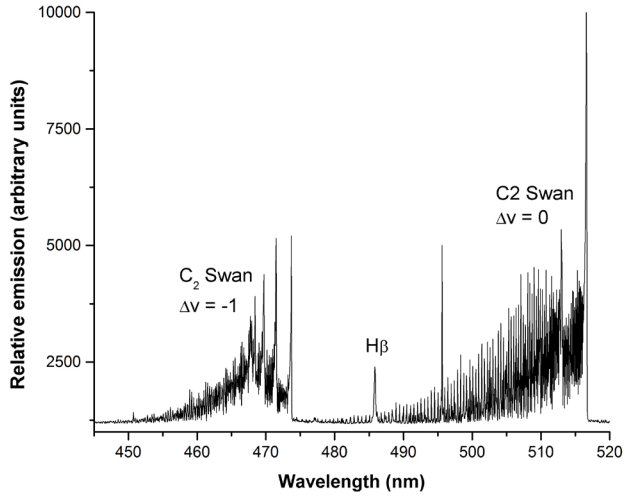

Figure 3: Stark broadening of the H_β line in reductive conditions in Run-9 recorded 70 mm beneath the torch.

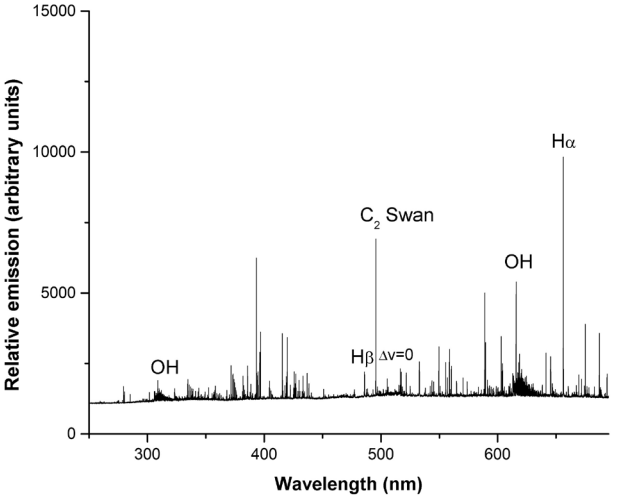

Figure 4: Optical emission spectra of the plasma during PVC decomposition in oxidative environment (Run-6), concentrating on the 250–700 nm region.

$$C + H_2 \rightarrow CH^* + H^* \quad (1)$$

We can assume this reaction route is not preferred in neutral conditions due to the consumption of hydrogen by chlorine atoms to form hydrogen chloride. Other reactions (Eqs. 2–4) between carbon and hydrogen can be accounted for several products from the thermodynamic calculations, such as CH_4, C_2H_2 and C_2H [33].

$$C + 2\,H_2 \rightarrow CH_4 \quad (2)$$

$$2\,C + H_2 \rightarrow C_2H_2 \quad (3)$$

$$C_2H_2 \rightarrow C_2H + H \quad (4)$$

Equilibrium calculations showed that all of these molecules are present in neutral conditions and their molar concentrations are intensified in reductive atmosphere. In oxidative conditions their formation is depressed. However, methane and acetone are too large to be observed by OES and the free C_2H radical has not been observed spectroscopically in the gaseous phase under laboratory conditions yet [34].

In oxidative conditions the signal intensity of CN and C_2 dropped considerably with the increasing oxygen concentration, while the observability of CH radical (Fig. 4) diminished. In the experiments conducted at high oxygen concentration the OH radical prevailed in the spectra. Excited OH radical (OH*) can be formed by the following chemiluminescence, reaction (Eq. 5):

$$CH + O_2 \rightarrow CO + OH^* \quad (5)$$

which reaction consumes the CH radicals in the plasma flame. There are other possible reaction routes for OH formations (Eqs. 6 and 7), but these are unlikely to occur in our system, because no decrease was observed in the intensity of hydrogen lines:

$$O + H \rightarrow OH^* \quad (6)$$

$$H + O_2 \rightarrow OH^* + O \quad (7)$$

The CN and C_2 features were much weaker away from the torch in each condition, while it was the opposite in case of OH. The CH band appeared only in spectra recorded closer to torch. In oxidative conditions the spectra taken here contained strong and broadened H_β lines and week OH features, while the detected emissions at 180 mm led to stronger OH features and very week or no H_β lines. These observed differences supported the assumption that close to the torch, in the high temperature zone, was the place where the PVC decomposed to its molecular fragments, while in the lower zone recombination of reactive radicals occurred.

In the 450–800 nm range continuous background was detected at the lower viewpoint. This background was the strongest between neutral conditions and was diminished by the introduction of auxiliary gases. It completely disappeared using oxygen at double stoichiometry. This phenomenon was caused by the emission of polycyclic aromatic hydrocarbon molecules and incandescent carbon nanoparticles with diameter around 40 nm.

Table 2: Identified radiative molecular systems.

Species	System	Wavelength (nm)	Transition
C_2	Swan	420 – 680	$d^3\Pi_g - a^3\Pi_u$
C_2	Deslandres – d'Azambuja	340 – 410	$C^1\Pi_g - A^1\Pi_u$
CH	3900 Å system	360 – 410	$B^2\Sigma - X^2\Pi$
CH	4300 Å system	410 – 440	$A^2\Delta - X^2\Pi$
CN	Violet	350 – 430	$B^2\Sigma - X^2\Sigma$
CN	2nd order Violet	700 – 900	$B^2\Sigma - X^2\Sigma$
OH	3064 Å system	300 – 360	$A^2\Sigma - X^2\Pi$
OH	2nd order band	600 – 670	$A^2\Sigma - X^2\Pi$
H_2	Fulcher α	590 – 640	$A^2\Pi - X^2\Sigma$

This phenomenon can also be observed in other plasma decomposition processes [22].

3.3 Determination of vibration-rotation temperatures

The vibration-rotation temperatures for C_2 Swan, CN violet and OH (A–X) bands were determined by a least-squares fitting program NMT applying the Nelder-Mead algorithm, developed at the University of Tennessee Space Institute [29,35-37]. The procedure is based on calculating the positions and the intensity of the transitions using an accurate quantum mechanical approach.

C_2, CN, OH vibration-rotation temperatures were determined under various experimental conditions and their values observed at 70 mm below the torch are given in Table 1. For the calculations more than 10 spectra were taken into account in each run. The error in the vibrational-rotational temperatures reported here was about ± 200 K. The standard deviations of relative intensity of the fit in most cases were below 0.2.

The temperatures observed in the window closer to the torch were always higher than in the other with at least 1500 K. For example in Run-1 it was 6400 K against 4000 K. Increasing the feed of PVC decreased the temperature of the C_2 bands because more energy was needed to the polymer decomposition. Due to similar reason the presence of auxiliary gases also decreased the Swan temperature. The decrease was smaller in reductive atmosphere than in oxidative, and was caused by the strong double bonds in the oxygen molecules. The OH band temperatures showed the same connections with the amount of presented oxygen. These connections could not be observed at the case of CN bands. The differences between the vibrational-rotational temperatures imply spatial distributions of the excitation and relaxation of the particular chemical species.

3.4 Solid product analysis

Representative TEM images on Fig. 5. show the products of neutral, oxidative and reductive experimental conditions, respectively. Only the typical plate like soot particles are present, no larger residual PVC grain can be observed, that implies full destruction of the feedstock material. Chlorine could be detected up to 1.4 atomic% by SEM-EDX measurement. This suggests that chlorine containing polycyclic aromatic hydrocarbons (PAHs) adsorbed on the surface of soot, which were also observed before in other thermal plasma decomposition processes [22]. The gas composition of the plasma had an influence on the size of soot particles. Without auxiliary gases the mean size was between 20 and 30 nm, while the presence of hydrogen increased it to 30–40 nm. However, in oxidative atmosphere it doubled and was around 60–80 nm. The ratio of Ar/H_2 or Ar/O_2 did not seem to have any observable influence on the end products. This phenomenon is also in agreement to former findings [22].

After purification with boiling H_2O_2 the soot on the TEM images showed similar patterns as the unpurified ones. There was no difference in the morphology or the organization of the individual particles. The "transparent thin paper structures" of graphene sheets [38] were not present and SAED measurement did not show any crystalline phase, only amorphous materials. Therefore we can assume no graphene growth from PVC precursor in thermal plasma.

4 Conclusions

Experimental investigations were performed for in-flight decomposition of PVC in RF thermal plasma reactor. The particular runs differed in the feed rate and the used auxiliary gases. In spite of the continuous feeding and the short residence time of PVC in the high temperature zone the decomposition was complete. The composition of the plasma column was modelled thermodynamically and was observed by OES. The temperatures of C_2, and OH vibrational-rotational bands were calculated and were measured in the 2000–6400 K range. Addition of oxygen or hydrogen decreased this value with more than a thousand K. Nitrogen was also present in the reactor due

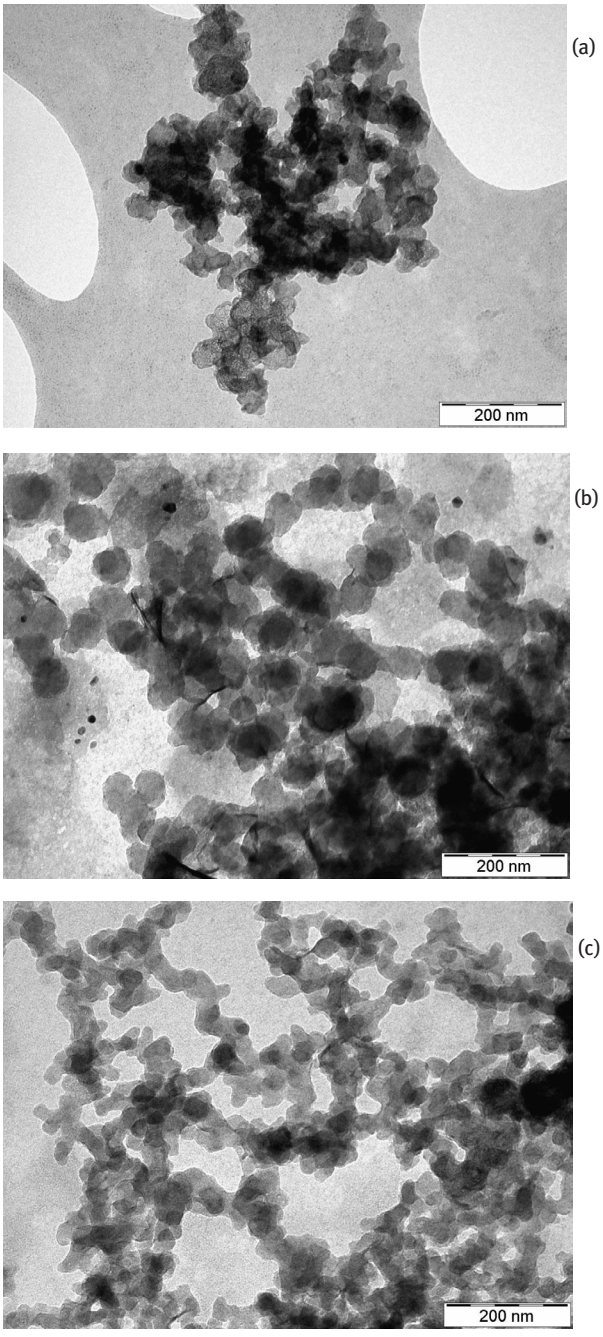

Figure 5: TEM micrographs of solid product sample from neutral (a), oxidative (b) and reductive (c) conditions.

to gas impurities or insufficient sealing but the formed CN molecules were useful thermometers owing to their high intensities at low concentrations. The possible graphene production during the plasma treatment was excluded by the TEM and SAED analysis of the purified soot samples.

Acknowledgement: This work has been supported by the National Development Agency (Grant No. KTIA_AIK_12-1-2012-0014). Thanks are expressed to Dr. James O. Hornkohl (University of Tennessee Space Institute) for providing us the NMT code.

References

[1] Saeki Y., Emura T., Technical progresses for PVC production, Prog. Poly. Sci., 2002, 27, 2055-2131

[2] Moulay S., Chemical modification of poly(vinyl chloride)—Still on the run, Prog. Poly. Sci., 2010, 35, 303-331

[3] Shadat-Shojai M, Bekhschandeh G.-R., Recycling of PVC wastes, Polym. Degrad. Stab., 2011, 96, 404-415

[4] Szarka Gy., Domján A., Szakács T., Iván B., Oil from poly(vinyl chloride): unprecedented degradative chain scission under mild thermooxidative conditionsPolym. Degrad. Stab., 2012, 97, 1787-1793

[5] Miranda R., Yang J., Roy C., Vasile C., Vacuum pyrolysis of PVC I. Kinetic study, Polym. Degrad. Stab., 1999, 64, 127-144

[6] Blazsó M., Jakab E., Effect of metals, metal oxides, and carboxylates on the thermal decomposition processes of poly(vinyl chloride), J. Anal. Appl. Pyrol., 1999, 49, 125-143

[7] Czégény Zs., Jakab E., Blazsó M., Thermal decomposition of polymer mixtures containing poly (vinyl chloride), Macromol. Mater. Eng., 2002, 287, 277-284

[8] Christmann W., Kasiske D., Klöppel K.D., Partscht H., Rotard W., Combustion of polyvinylchloride- an important source for the formation of PCDD/PCDF, Chemosphere, 1989, 19, 387-392

[9] Mohai I., Gál L., Szépvölgyi J., Gubicza J., Farkas Z., Synthesis of nanosized zinc ferrites from liquid precursors in RF thermal plasma reactor, J. Eur. Chem. Soc., 2007, 27, 941-945

[10] Guddeti R.R., Knight R., Grossmann E.D., Depolymerization of polyethylene using induction-coupled plasma technology, Plasma Chem. Plasma Proc., 2000, 20, 37-64

[11] Föglein K.A., Szabó P.T., Dombi A., Szépvölgyi J., Comparative study of the decomposition of CCl4 in cold and thermal plasma, Plasma Chem. Plasma. Proc., 2003, 23, 651-664

[12] Föglein K.A., Szabó P.T., Babievskaya I.Z., Szépvölgyi J., Comparative Study on the decomposition of chloroform in thermal and cold plasma, Plasma Chem. Plasma. Proc., 2005, 25, 289-302

[13] Todorovic-Markovic B., Markovic Z., Mohai I., Károly Z., Gál L., Föglein K., Szabó P.T., Szépvölgyi J., Efficient Synthesis of fullerenes in RF Thermal Plasma reactor, Chem. Phys. Lett., 2003, 378, 434-439

[14] Cota-Sanchez G., Souczy G., Huczko A., Lange H., Fullerenes and Nanotubes Using Carbon Black-Nickel Particles, Carbon, 2005, 43, 3153-3166

[15] Shahverdi A., Souczy G., Counter-current ammonia injection flow during synthesis of single-walled carbon nanotubes by induction thermal plasma, Chem. Eng. Sci., 2013, 104, 389-98

[16] Choi S.I., Nam J.S., Lee C.M., Choi S.S., Kim J.I., Park J.M., Hong S.H., High purity synthesis of carbon nanotubes by methane decomposition using an arc-jet plasma, Curr. Appl. Phys., 2006, 6, 224-229

[17] Horii N., Suzuki N., Itoh K., Kotaki T., Matsumo O., Deposition of diamond from plasma jets with chlorobenzenes as carbon source, Diam. Relat. Mater., 1997, 6, 1874-1882

[18] Aso H., Matsuoka K., Sharma A., Tomita A., Structural analysis of PVC and PFA carbons prepared at 500–1000 °C based on elemental composition, XRD, and HRTEM, Carbon, 2004, 42, 2963-2973

[19] Nemes L., Irle S., Spectroscopy, dynamics and molecular theory of carbon plasmas and vapours, World Scientific Publishing, Abingdon, 2009

[20] Al-Shboul K.F., Harilal S.S., Hassanein A., Polek M., Dynamics of C2 formation in laser-produced carbon plasma in helium environment, J. Appl. Phys., 2011, 109, 053302

[21] Nemes L., Keszler A.M., Hornkohl J.O., Parigger C.G., Laser-induced carbon plasma emission spectroscopic measurements on solid targets and in gas-phase optical breakdown, Appl. Opt., 2005, 44, 3661-3667

[22] Fazekas P., Bódis E., Keszler A.M., Czégény Zs., Klébert Sz., Károly Z., Szépvölgyi J., Decomposition of chlorobenzene by thermal plasma processing, Plasma Chem. Plasma. Proc., 2013, 33, 765-778

[23] Kramida. A., Ralchenko, Y., Reader J., and NIST ASD Team, NIST Atomic Spectra Database (ver. 5. 1.), 2013, http://physics,nist.gov/asd

[24] [24] Luque J., Crosley D.R., LIFBASE, Database and Spectral Simulation for Diatomic Molecules, SRI International, Menlo Park, CA, USA, 1999

[25] Pearse R.W.B., Gaydon A.G., The identification of molecular spectra, 4th edition, Chapman and Hall, London, 1976

[26] Hertzberg G., Molecular Spectra and Molecular Structure, D Van Nostrand Company, Inc., New Jersey, 1950

[27] Wallace L., Astrophys. J. Suppl., 1962, 7, 165

[28] Bystrzejewski M., Rümmeli M.H., Gemming T., Lange H., Huczko A., Catalyst-free synthesis of onion-like carbon nanoparticles, New Carbon Mater., 2010, 25, 1-8

[29] Parigger C.G., Plemmons D.H., Oks E., Balmer Series H-beta measurements in a laser-induced hydrogen plasma, Appl. Opt., 2003, 42, 5992-6000

[30] King A.S., Swings P., Astrophys. J., 1945, 101, 6

[31] Babánková D., Civis S., Juha L., Bitter M., Cihelka J., Pfeifer M., Skála J., Bartnik A., Fiedorowicz H., Mikolajczyk J., Ryc L., Sedicová T., Optical and X-ray emission spectroscopy of high-power laser-induced dielectric breakdown in molecular gases and their mixtures, J. Phys. Chem. A, 2006, 110, 12113-12120

[32] Dean, A.J., Davidson D.F., Hanson R.K., A shock tube study of reactions of carbon atoms with hydrogen and oxygen using excimer photolysis of C3O2 and carbon atom atomic resonance absorption spectroscopy, J. Phys. Chem., 1991, 95, 183-191

[33] Baddour, R.F., Iwasyk, J.M., Reactions between elemental carbon and hydrogen at temperature above 2800 K, Ind. Eng. Chem. Process. Des. Dev. 1962, 1, 169-176

[34] Reitblat A.A., Soviet Astronomy Letters, 1980, 6, 406

[35] Hornkohl J.O., Parigger C.G., Lewis J.W.L., Temperature Measurements from CN Spectra in a Laser-Induced Plasma, J. Quant. Spectrosc. Radiat. Transf., 1991, 46, 405-411

[36] Parigger C.G., Plemmons D.H., Hornkohl J.O., Lewis J.W.L., Spectroscopic Temperature Measurements in a Decaying Laser-Induced Plasma using the C2 Swan System, J. Quant. Spectrosc. Radiat. Transf., 1994, 52, 707-711

[37] Parigger C.G., Hornkohl J.O., Keszler A.M., Nemes L., Measurement and analysis of OH emission spectra following laser-induced optical breakdown in air, Appt. Opt., 2003, 42, 6192-6198

[38] Tong X., Wang H., Wang G., Wan L., Ren Z., Bai J., Bai J., Controllable synthesis of graphene sheets with different numbers of layers and effect of the number of graphene layers on the specific capacity of anode material in lithium-ion batteries, J. Solid State Chem., 2011, 184, 982-989